Spin states of iron impurities in magnesium oxide under pressure: A possible intermediate state

R. Larico,[1] L. V. C. Assali,[2] and J. F. Justo[1]

[1]*Escola Politécnica, Universidade de São Paulo, CP 61548, CEP 05424-970, São Paulo, SP, Brazil*

[2]*Instituto de Física, Universidade de São Paulo, CP 66318, CEP 05315-970, São Paulo, SP, Brazil*

(Received 12 June 2012; revised manuscript received 27 December 2012; published 8 April 2013)

Ferropericlase (Mg,Fe)O is a major lower mantle mineral, and studying its properties is a fundamental step toward understanding the Earth's interior. Here, we performed a first-principles investigation on the properties of iron as an isolated impurity in magnesium oxide, which is the condition of ferropericlase under which iron-iron interactions could be neglected. The calculations were carried using the all-electron full-potential linearized augmented plane wave method within the density functional theory in the generalized gradient approximation plus the on-site Hubbard correction. We present the electronic and magnetic properties, electric and magnetic hyperfine splitting of this impurity in high and low spin states for several charge states at zero pressure, which were then extended to high pressures. For the impurity in the neutral charge state, our results indicated that there is a metastable intermediate spin state ($S = 1$), in addition to the high ($S = 2$) and low ($S = 0$) spin states. Those results were discussed in the context of an intermediate spin state, experimentally identified in ferrosilicate perovskite.

DOI: 10.1103/PhysRevB.87.165113 PACS number(s): 91.60.Pn, 75.30.Kz, 81.40.Rs

I. INTRODUCTION

The identification of a pressure induced iron high-to-low spin transition in ferropericlase, $(Mg_{1-x}Fe_x)O$,[1] and ferrosilicate perovskite ($Mg_{1-x}Fe_xSiO_3$)[2] has stimulated investigations on several aspects of this transition.[3–10] Since those are the two major minerals in Earth's lower mantle and the respective iron spin transitions were observed in mantle thermodynamic conditions, important geophysical implications could be anticipated, in terms of mantle chemical composition, heterogeneity, elasticity, and radiative transmission.[11]

In ferropericlase, an iron atom stays in a substitutional magnesium site, donating two valence electrons to its nearest neighboring oxygen atoms. The six remaining $3d$-iron-related electrons generate a $t_2 + e$ pair of orbitals in the crystalline field, with the t_2 orbital below the e one. At low pressures, the exchange splitting prevails over the crystalline field one, favoring the high spin (HS) $S = 2$ state. With increasing pressure, the crystalline field splitting becomes more important, favoring the low spin (LS) $S = 0$ state beyond a certain transition pressure. Early experiments at room temperature[3] have suggested that this transition should be very sharp, occurring in a narrow pressure range. On the other hand, more recent theoretical[6,9,10] and experimental[7,12,13] investigations showed that it should be smoother, across wide pressure and temperature ranges. The current model for this transition describes ferropericlase as a solid solution with simultaneous concentrations of iron atoms in HS and LS states, which are determined by the thermodynamic conditions of the material.[9,10]

The phenomenology of iron in mantle minerals is very rich, and a proper investigation on its properties is a fundamental step to build compositional models for the Earth's interior. However, there are many open questions that still need to be addressed in order to understand the implications of the spin transition for the mantle physical properties. For example, there are several conflicting results in the literature concerning the elasticity of ferropericlase across this transition.[12–15] Another important element concerns the radiative conductivity of the mineral across the spin transition,[5,16] since such knowledge may help to build better temperature profiles of the Earth's lower mantle and core. There is also considerable uncertainty on the pressure range of that spin transition. While earlier experiments[1,3–5] indicated that it occurred in the 30–40 GPa pressure range, at room temperature, more recent investigations suggested higher pressures for such transition.[16–18]

An equivalent high-to-low spin transition has been observed for iron in ferrosilicate perovskite,[2,8] the most abundant lower mantle mineral. An intriguing result is that while for iron in ferropericlase, only two spin states have been identified so far, in ferrosilicate perovskite, an intermediate ($S = 1$) spin state has also been observed.[8] This leads directly to the question whether this intermediate spin state could be also energetically favorable in ferropericlase. Several other questions are also open, such as the concentration of available electrons in the lower mantle, as result of intrinsic or extrinsic defects in those minerals. This is an important property that could help to determine the charge state of iron atoms in minerals at those depths. Here, we present a theoretical investigation that explores some of those questions, considering the case of an isolated iron atom in magnesium oxide. In that case, iron was modeled as an impurity, such that the effects of iron-iron interactions could be neglected, and we could focus only on the properties of an isolated iron center. The first-principles calculations were performed using the all-electron full-potential linearized augmented plane wave method, within the density functional theory and the generalized gradient approximation plus the on-site Hubbard correction in the $3d$-related iron states. The introduction of this potential, computed self-consistently, was a fundamental step to provide an appropriate description on the iron-related electronic energy levels. We computed the structural, electronic, and magnetic properties of iron in several charge states, and the respective electric and magnetic hyperfine splitting parameters of active centers. We then investigated the pressure effects on those properties, and compared our results to available experimental data.

II. METHODOLOGY

The calculations were performed within the density functional theory, using the all-electron full-potential linearized augmented plane wave (FP-LAPW) method, implemented in the WIEN2K package.[19] The electronic exchange interaction was described within the generalized gradient approximation[20] plus the Hubbard U potential correction (GGA + U).[21] The on-site U values for the iron $3d$ states were obtained self-consistently using the methodology described by Madsen and Novák.[22]

We considered a 54-atom MgO rocksalt reference supercell in which an iron atom was placed in a substitutional magnesium site. The irreducible Brillouin zone was sampled by a grid of $2 \times 2 \times 2$ k points. Convergence on the total energy of the system was achieved using a $7.0/R$ parameter, which defines the total number of plane waves to describe the electronic wave functions in the interstitial regions, where R is the sphere radius of all the atomic regions ($R = 0.90$ Å). For a certain atomic configuration, self-consistent iterations were performed until reaching convergence on both the total energy (10^{-4} eV/atom) and the total charge in the atomic spheres (10^{-5} electronic charges/atom). The positions of all atoms were relaxed, with no symmetry constrains, until the forces were smaller than 0.02 eV/Å in any atom. In order to get results for different spin state configurations, some simulations were performed with constrained spin states.

The formation energy of a charged iron impurity in MgO, $E_f^q(\mathrm{MgO:Fe_{Mg}})$, is defined as[23]

$$E_f^q(\mathrm{MgO:Fe_{Mg}}) = E_{\mathrm{tot}}^q(\mathrm{MgO:Fe_{Mg}}) - E_{\mathrm{tot}}(\mathrm{MgO}) + \mu_{\mathrm{Mg}} - \mu_{\mathrm{Fe}} + q(\epsilon_v + \varepsilon_F),$$

where $E_{\mathrm{tot}}^q(\mathrm{MgO:Fe_{Mg}})$ is the total energy of a supercell, in the q charge state, containing the substitutional iron impurity, $E_{\mathrm{tot}}(\mathrm{MgO})$ is the total energy of a MgO crystal considering the same reference supercell. Additionally, ϵ_v is the valence band top, adjusted to the band structures of the bulk material with and without the impurities, for each q charge state.[23,24] This correction in the valence band top is necessary, due to inhomogeneities in the charge density of the finite primitive cell, which causes a Coulomb multipole interaction with its images, as discussed in Ref. 25. Additionally, a uniform jellium background was implicitly considered to cancel out the long range multipole interactions of charged supercells.[23] ε_F is the Fermi level, μ_{Fe} and μ_{Mg} are, respectively, the Fe and Mg chemical potentials, computed within the same methodology described earlier, for the stable metallic crystalline phases. All the approximations and convergence criteria presented in the previous paragraphs have been shown to provide an accurate description on the electronic and structural properties of defect centers in a number of materials.[26–28]

The introduction of a Hubbard potential correction represented a crucial element for an appropriate description of the $3d$-iron-related states in ferropericlase and iron oxide,[6] and consequently in the systems studied here. It is well established in the literature that the density functional theory provides a poor description of the strongly correlated electronic systems, such as the $3d$-iron-related levels in the systems discussed here. The calculations with the local density or generalized gradient approximations lead to a metallic state for ferropericlase or iron oxide, although experimental results indicate that those systems are insulators.[6] The introduction of a Hubbard on-site correction increased the correlation interactions of $3d$-related electronic levels, providing results more consistent with the available experimental data. There are several procedures to compute the Hubbard potential and, over the last few years, several U values have been used for those systems.[6,29] On the other hand, our investigation computed this potential self-consistently.[22]

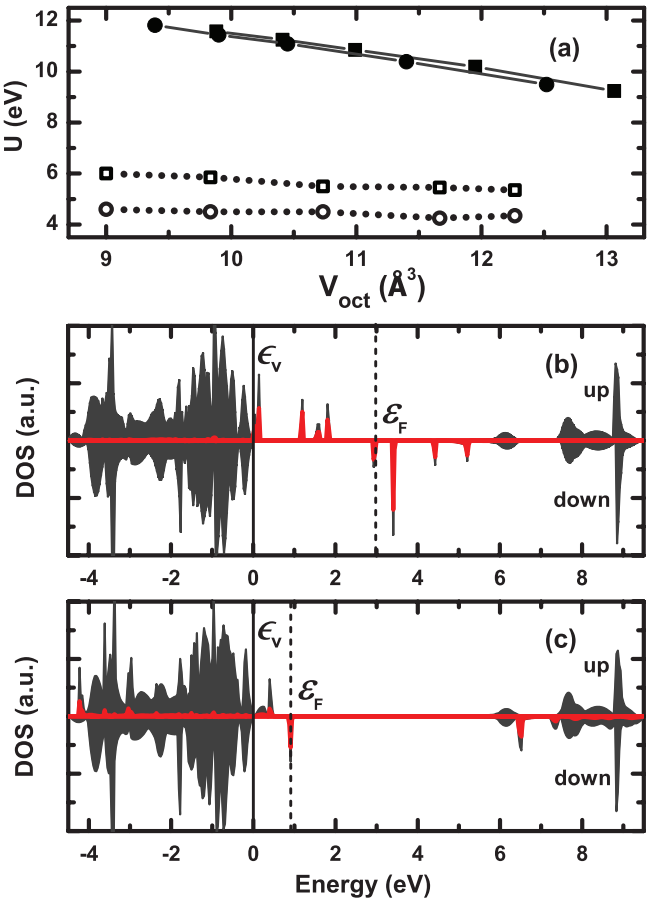

FIG. 1. (Color online) (a) Computed on-site Hubbard U values for the $3d$ states, as a function of the volume of the oxygen octahedral around the iron atoms, for HS (squares) and LS (circles) configurations. Our results (full symbols) are compared to those of other theoretical investigations (open symbols).[6] (b) and (c) show the total density of states (TDOS) (dark gray regions) and partial density of states (PDOS) (solid lines in red) projected in the Fe $3d$-related energy levels of the HS state, without and with the correction, respectively. The spin up (down) states are represented in top (bottom) of the figs. (b) and (c). Additionally, the energy reference is set at the valence band top of MgO ($\epsilon_v = 0$), and the dashed lines represents the highest occupied level.

Figure 1(a) shows the values of the Hubbard potential as a function of the volume of the oxygen octahedron around the iron atom, as compared to the values used by other authors for ferropericlase. Only for reference, some authors used constant values (3 or 5 eV) for the Hubbard potential irrespective of the octahedral volume.[29] The self-consistent values used here are considerably larger than the ones from other calculations. However, it should be pointed out that the value of this potential

depends strongly on the methodology: while our calculations were performed within the full potential method (FP-LAPW), others were performed within the pseudopotential method.[30] For example, in the Fe_2O_3 system, the iron Hubbard potential was found to be 8.73 eV within a full potential calculation[22] and 3.3 eV within a pseudopotential calculation.[31] Additionally, other recent theoretical investigations have also used large U values for the $3d$-related energy levels of iron,[22,32,33] consistent with our values.

Figures 1(b) and 1(c) show respectively the density of states of the system without and with the correction, indicating that it provides an appropriate description of the electronic structure. Without the correction, the energy difference between the highest occupied and lowest unoccupied iron-related levels was 0.5 eV. This energy difference changed to 5.5 eV with the correction.

III. RESULTS

A. Zero-pressure results

Under ambient conditions, MgO crystallizes in the rocksalt (B1) structure, with a measured lattice parameter of $a_{\text{expt}} = 4.216$ Å, presenting a large direct electronic band gap of 7.67 eV.[34] In this study, using the approximations presented in the previous section, we found an equilibrium lattice parameter of $a_{\text{th}} = 4.21$ Å and a direct band gap of $E_g = 4.50$ eV. Those values are consistent with values from other theoretical investigations using similar approximations[35] and in a good agreement with experimental data.[34]

We considered several charge and spin states for the substitutional iron impurity, using the supercell with the MgO theoretical lattice parameter. We computed the formation and transition energies, along with the respective structural and electronic properties of HS and LS states. For a certain charge state, in order to build an energy stability curve as a function of iron magnetic moments, we performed a set of calculations constraining the total spin of the system.

Table I presents the properties of the impurity in several q charge states, $(\text{MgO} : \text{Fe}_{\text{Mg}})^q$. The presence of a substitutional Fe impurity in MgO caused important relaxations on the neighboring oxygen atoms. For the impurity in the neutral charge state in its HS, the system presented an outward relaxation with respect to the original MgO crystalline structure. The volume of the oxygen octahedron around a Mg atom was 12.81 Å^3 in MgO, while with the substitutional iron impurity in its HS state it changed to 13.45 Å^3. This outward relaxation hides an important symmetry lowering, due to a Jahn-Teller distortion, as result of the iron-related partially occupied electronic energy levels. Going from this HS state to the LS one, there was a substantial inward relaxation, with the volume of the oxygen octahedron going to 13.08 Å^3, representing a 3% volume reduction with respect to that in the HS state. Additionally, since the LS state presented a full shell electronic occupation, it had an octahedral symmetry. This volume reduction was in reasonably good agreement with the 7% reduction, computed in another theoretical investigation on ferropericlase ($Mg_{1-x}Fe_xO$ with $x = 0.1875$.[6] The calculations for that alloy allowed crystalline relaxation with the presence of Fe, while our calculations considered a fixed MgO lattice, justifying a smaller inward relaxation on the octahedron. According to Table I, for the positive and doubly positive charge states, there were also substantial inward relaxations going from a HS to a LS state. Additionally, for a certain spin state (HS or LS), the octahedron became smaller as going from a neutral charge state to positive or doubly positive ones.

We found that Fe was stable only in three charge states (neutral, positive, and doubly positive), presenting $3d$-related energy levels in the MgO band gap. For the neutral charge state, we computed the properties of the HS and LS states, and found that the formation energy of the HS state is 1.44 eV lower than that of the LS one. Consistent with theoretical[6,9] and experimental[3,4] results for ferropericlase, our results indicated that the HS state is considerably more stable than the LS one at low pressures. For the positive charge state, there are also the HS and LS states, corresponding to 5/2 and 1/2 spin values. Here, the formation energy of the HS state is 2.12 eV lower than the LS one. For the doubly positive charge state, there are also the HS and LS states, respectively, with $S = 2$ and 1, with the HS state having lower formation energy than the LS one. The results indicated that, for low pressures, the HS state was more stable than the LS one, irrespective of the charge state of the center.

Figure 2 shows the formation energy of the $(\text{MgO} : \text{Fe}_{\text{Mg}})^q$ center at several q charge states as a function of the MgO Fermi level ($0 \leqslant \varepsilon_F \leqslant E_g$), where the valence band top was set to zero ($\epsilon_v = 0$) and E_g is the materials band gap. For the HS

TABLE I. Results for isolated substitutional Fe impurities in MgO at zero pressure: spin state configuration, total spin (S), the localized magnetic moment inside the atomic iron sphere (μ_B^{Fe}), the volume of the oxygen octahedron around the Fe atom (V_{oct}), formation (E_{f}), and transition (E_t) energies for several q charge states, and magnetic hyperfine parameters (A_1, A_2, and A_3). The transition energies were computed with respect to the MgO valence band top (ϵ_v), as discussed in the text. Volumes, magnetic moments, energies, and hyperfine parameters are given, respectively, in Å^3, Bohr magneton, eV, and MHz.

Center	State	S	μ_B^{Fe}	V_{oct}	E_{f}	E_{t}	A_1	A_2	A_3
$(\text{MgO} : \text{Fe}_{\text{Mg}})^0$	HS	2	3.44	13.45	10.14		9	28	28
	IS	1	1.73	13.30	11.41		−20	49	38
	LS	0	0.0	13.08	11.58		0	0	0
$(\text{MgO} : \text{Fe}_{\text{Mg}})^+$	HS	5/2	4.13	12.02	$6.31 + \varepsilon_F$	3.83 (+/0)	20	20	20
	IS	3/2	2.80	11.67	$9.73 + \varepsilon_F$	1.68 (+/0)	−7	34	34
	LS	1/2	0.98	11.20	$8.43 + \varepsilon_F$	3.15 (+/0)	4	36	22
$(\text{MgO} : \text{Fe}_{\text{Mg}})^{2+}$	HS	2	4.12	11.94	$5.53 + 2\varepsilon_F$	0.78 (2+/+)	25	25	25
	LS	1	2.55	10.45	$6.31 + 2\varepsilon_F$	2.12 (2+/+)	−5	38	38

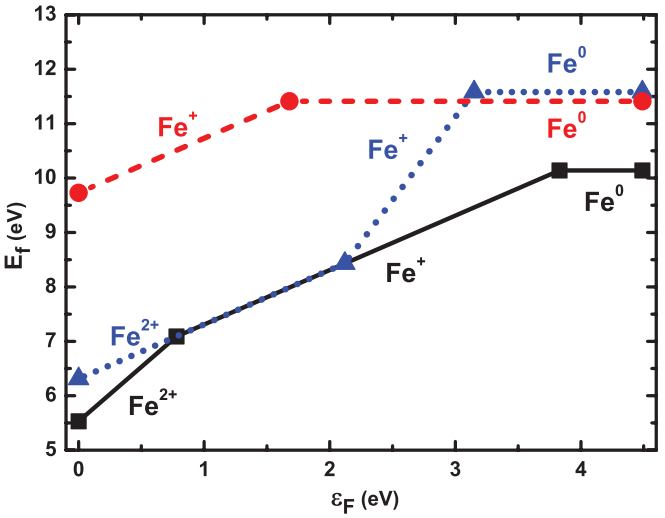

FIG. 2. (Color online) Formation energies of $(MgO:Fe)^q$ as a function of Fermi energy position in the MgO bandgap for the isolated impurity. The zero of Fermi level corresponds to the valence band top. Square, triangle, and circle symbols correspond, respectively, to HS, LS, and IS states at zero pressure.

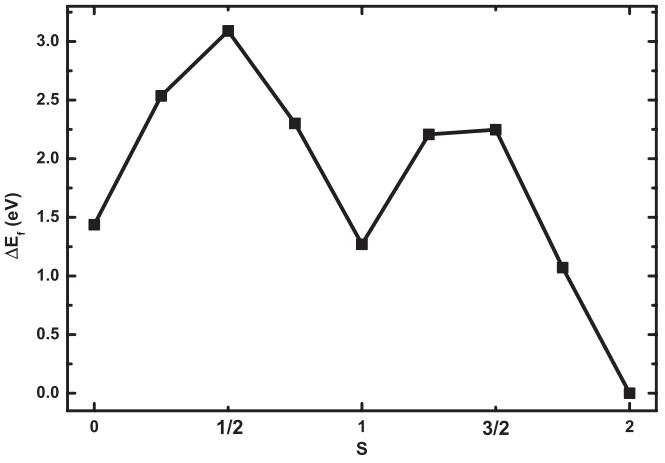

FIG. 3. Total energy difference (ΔE), with respect to the total energy of the HS ground state, of $(MgO : Fe_{Mg})^0$ as a function of the spin of the center (S) at zero pressure. The solid lines are only a guide to the eyes.

state, the doubly positive charge state is stable for $0 \leqslant \varepsilon_F \leqslant 0.78$ eV, the positive charge state is stable for $0.78 \leqslant \varepsilon_F \leqslant 3.83$ eV, while the neutral one is stable for $\varepsilon_F > 3.83$ eV. According to Fig. 2, since formation energy of the LS state is higher than the one of the HS state, the stability curve corresponding to the LS state is over the curve corresponding to the HS one for any value of the Fermi level. Since the density functional theory calculations underestimate the MgO band gap by more than 3 eV, when compared to experimental data,[34] as discussed earlier, then the neutral charge state, $(MgO : Fe_{Mg})^0$, is expected to be the stable configuration for the Fermi level lying in the top half part of the MgO band gap.

We also computed the energy barrier, as a function of the total magnetic moment, for the systems going from a HS toward a LS state. In order to perform such analysis, the energetics of the systems were computed with constrained intermediate magnetic moments between the HS and LS configurations, in the neutral charge state. Figure 3 presents the total energy, of the neutral charge state, as a function of spin configurations of the centers between $S = 0$ and 2 states. The results indicated that going from a HS state to a LS one, there was a metastable intermediate spin (IS) state, with $S = 1$. The Hubbard potential value of the IS state is essentially the same of the HS one. This IS state had a total energy of about 1.30 eV higher than that of the HS state, and even a little smaller than the LS one. This IS state had a volume of the oxygen octahedron of 13.30 $Å^3$, which is a little smaller than that of the HS state (of 13.45 $Å^3$). The presence of an intermediate spin state was carefully explored in order to check if it was not only a theoretical artifact. In order to explore this IS state, we performed calculations with several U values (from 0 to 9 eV), and we found that the IS state is metastable in all those cases. Additionally, we performed calculations with unconstrained magnetic moments around $S = 1$ (with $S = 0.75$ and 1.25), and both calculations converged toward the IS state with $S = 1$. For the positive charge state, we also observed an IS state in a metastable configuration, while for the doubly positive one, we found no IS state.

At zero pressure, the large difference in total energies, for the neutral charge state, indicated that essentially all the iron centers would be in the HS state. Considering the solid solution model with concentrations of HS and LS states,[9,10] our results indicated that there would be very small concentrations of LS and IS states at low pressures,[36] even at high temperatures. The energy barriers for the spin crossover are very large for both the HS-IS and IS-LS transitions. Here, we should point out that the introduction of a Hubbard potential, to provide a proper description of the electronic structure of the system, comes with a price: a poorer description of the total energy of the system. Several attempts have been introduced in the literature to improve the description of the total energy.[37] Therefore there are important uncertainties in the energy barriers for the spin crossover.

We also found that the IS configuration is a possible spin state for Fe in ferropericlase, and is fully consistent with the experimental observation of an equivalent IS state in ferrosilicate perovskite.[8] However, the small difference in the oxygen octahedron volume, between the HS and IS states, may hamper an identification of this center in ferropericlase using several experimental methodologies. A possible way to identify such center is by electron paramagnetic resonance (EPR) spectroscopy, in which the hyperfine parameters could be measured. Table I presents the magnetic hyperfine parameters for all the electrically active iron centers in MgO at zero pressure. For the $(MgO : Fe_{Mg})^0$ center, the differences in those parameters for HS and IS states may allow an identification of this IS state by EPR measurements.

The difference in the electronic structure between the HS and IS states could also help identifying such IS state. Figure 4 presents the electronic structure of the $3d$-iron-related energy levels in $(MgO : Fe_{Mg})^0$ for the HS, IS, and LS states. In the LS state, the system consists of only $t_2 + e$ levels in a close shell configuration. The t_2 level is fully occupied near the valence band top of MgO and the e one is unoccupied in the conduction band. For the HS state, due to the symmetry

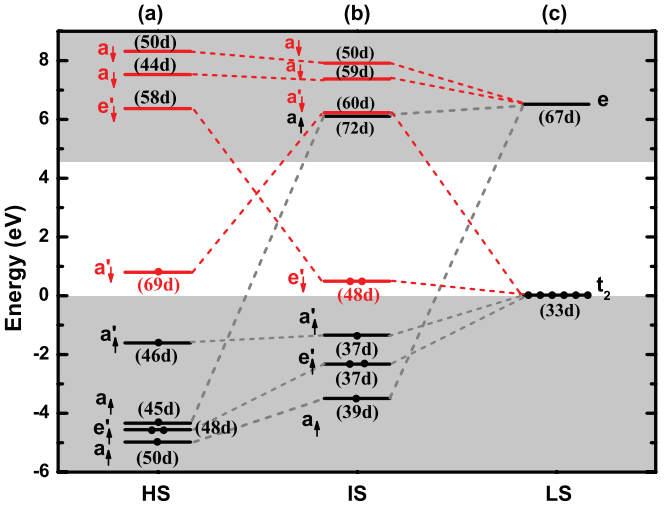

FIG. 4. (Color online) The Kohn-Sham spin-polarized energy eigenvalues around the Γ point, representing the 3*d*-related Fe levels around the gap region for isolated substitutional neutral Fe in several spin configurations: (a) $S = 2$ (HS), (b) 1 (IS), and (c) 0 (LS). The gap level occupations are given by the numbers of filled circles. Numbers in parentheses represent the *d*-character percentage of charge inside the Fe atomic sphere. Up and down arrows represent the spin up and spin down levels, respectively.

lowering, in comparison to the LS state, the t_2 level splits into $a + e$ levels. The HS state consists of five electrons with spin up and one with spin down. The last occupied level is an $a_\downarrow$ orbital, with 69% of *d* character (inside the Fe sphere), about 1 eV higher than the valence band top of MgO. Finally, the IS state has the highest occupied level as an $e_\downarrow$ with two electrons, and with 48% of *d* character. This level is near the valence band top, while the first unoccupied level is inside the conduction band.

B. High-pressure results

A possible way to explore the properties of iron impurities in MgO is observing the pressure effects. This would be specially important to identify the IS state, using EPR or Mösbauer spectroscopies.

First of all, in order to provide consistent results for MgO under pressure, we explored the elastic properties of MgO. Our calculations indicated a bulk modulus of 152 GPa, using a third-order Birch-Murnaghan equation of state, which is fully consistent with the values obtained by other theoretical investigations using similar approximations[35] and in excellent agreement with experimental data.[34] This equation of state was later used to obtain the dependence of the MgO lattice parameter with external pressure.

An important property is to check the stability of the spin states as a function of pressure. In ferropericlase, high to low spin transition has been observed in the 30–50 GPa range at room temperature, depending on the concentration of iron in the material.[38,39] For very low iron concentrations, it has been found a transition near 30 GPa. In order to check the stability of the spin states of iron atoms in MgO, we computed the respective enthalpy of formation as a function of pressure for different spin states at the neutral charge state.

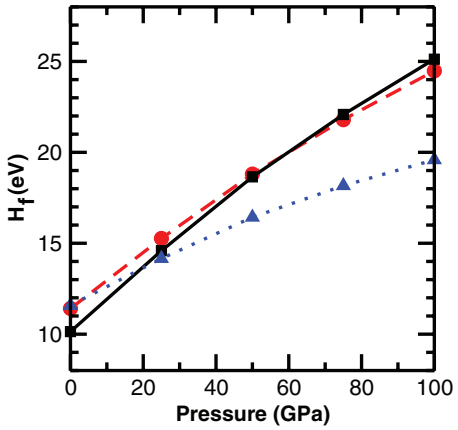

FIG. 5. (Color online) Enthalpy of formation (H_f) of iron impurity in magnesium oxide in the neutral charge state, $(MgO : Fe_{Mg})^0$, as a function of pressure at different spin states. Square, triangle, and circle symbols correspond respectively to HS, LS, and IS states.

In order to obtain the enthalpy of formation, we computed the respective volumes of formation, following the procedure used in other systems.[40] Figure 5 shows the enthalpy of formation as a function of pressure for iron in MgO. The results indicated that the HS and LS curves cross each other at about 20 GPa, indicating an spin transition. This result is fully consistent with experimental data for ferropericlase at low iron concentrations.[39] The figure also shows that across the pressure range, the IS is always higher in energy than other spin states.

We observed that, for all charge states, the external pressure does not modify the point symmetry of the centers, only compressing the respective oxygen octahedra. Therefore pressure modifies only slightly the center structures, affecting more strongly the electronic structures, as the energy levels are shifted with respect of the materials band gap.

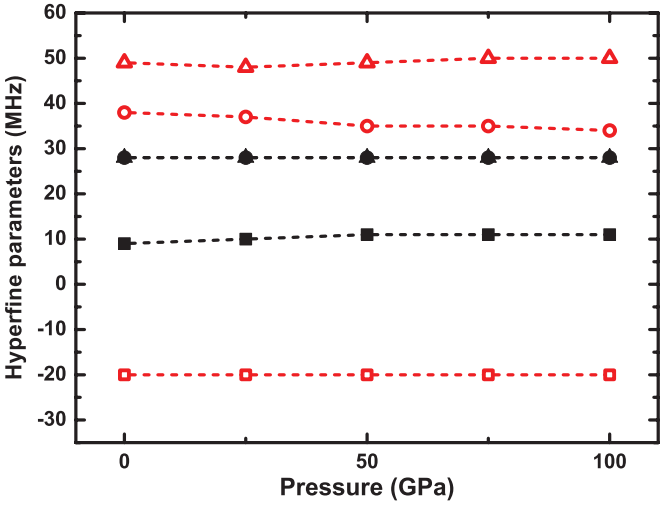

FIG. 6. (Color online) Magnetic hyperfine parameters: A_1 (squares), A_2 (triangles), and A_3 (circles) for the $(MgO : Fe_{Mg})^0$ center, in HS (close symbols) and IS (open symbols) states, as a function of pressure. The pressure, as a function of the lattice parameter, was computed considering the fitting of a third-order Birch-Murnaghan equation of state.

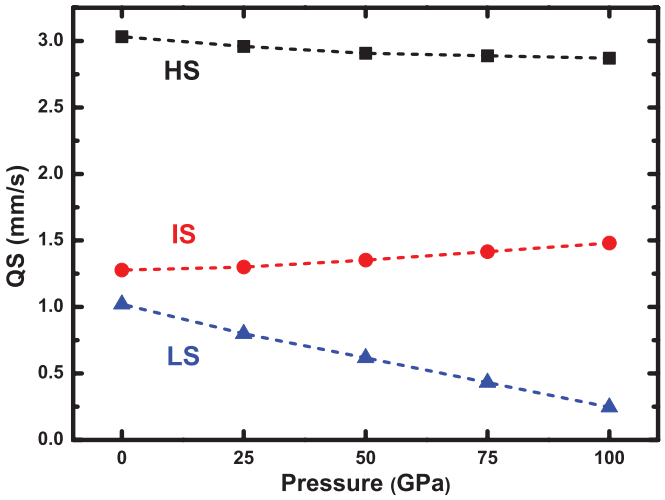

FIG. 7. (Color online) Quadrupole splitting (QS) of $(MgO : Fe_{Mg})^0$ center in HS (squares), IS (circles), and LS (triangles) states as a function of pressure.

Figure 6 presents the theoretical magnetic hyperfine parameters for the HS and IS states in the neutral charge state as a function of pressure. The large differences in the hyperfine parameters, between HS and IS states, may allow a proper identification of this IS state in ferropericlase. The figure also shows that those parameters are essentially insensitive to external pressure.

Nuclear quadrupole resonance is another technique that could allow to distinguish the HS and IS states, in which the measurements are associated to the electric field gradient (EFG) of each center. We computed the EFG of all spin states in the $(MgO : Fe_{Mg})^0$ as a function of pressure. The computed electric field gradient, V_{zz}, at the center of the iron nucleus is converted to the quadrupole splitting (QS) value, using the relation $QS \simeq eQV_{zz}/2h$, where $h/e = 4.1356692 \times 10^{-15}$ V/MHz and Q denotes the nuclear electric quadrupole moment of iron. The EFGs were converted to the QS values using the ^{57}Fe nuclear quadrupole moment of $Q = 0.16 \pm 0.02$ barn (1 barn $= 10^{-28}$ m^2).[41] Figure 7 shows the QS of the $(MgO : Fe_{Mg})^0$ center as a function of pressure in the HS, IS, and LS configurations. The QS is very sensitive to increasing external pressure, decreasing for the HS state, while increasing for the IS one, which may help to distinguish the HS and IS states.

Figure 8 compares the theoretical QS values for the $(MgO : Fe_{Mg})^q$, in several charge states with the values of an iron atom in ferrosilicate perovskite, represented as the $(MgSiO_3 : Fe_{Mg})^0$ center in the figure, obtained by recent theoretical[42] and experimental[43] investigations. Ferrosilicate perovskite has two different sites for iron. As a result, for the $(MgSiO_3 : Fe_{Mg})$ center, in the neutral charge state, the iron atom can stay in two net charge states (2+ or 3+), depending on the lattice site, meaning that iron can donate two or three electrons to its neighboring oxygen atoms. According to the figure, the $(MgO : Fe_{Mg})^0$ center has QS values, for all three spin states, that are consistent with the respective ones associated to the iron in a 2+ oxidation state (Fe^{2+}) in ferrosilicate perovskite. This provides an additional confirmation that the iron atom in MgO in a neutral charge state, $(MgO : Fe_{Mg})^0$, has a 2+ oxidation charge state, i.e., it donates two electrons to its neighboring oxygen atoms. On the other hand, the $(MgO : Fe_{Mg})^+$ center has QS values, for all three spin states, that are consistent with the respective ones associated to the iron Fe^{3+} in ferrosilicate perovskite,

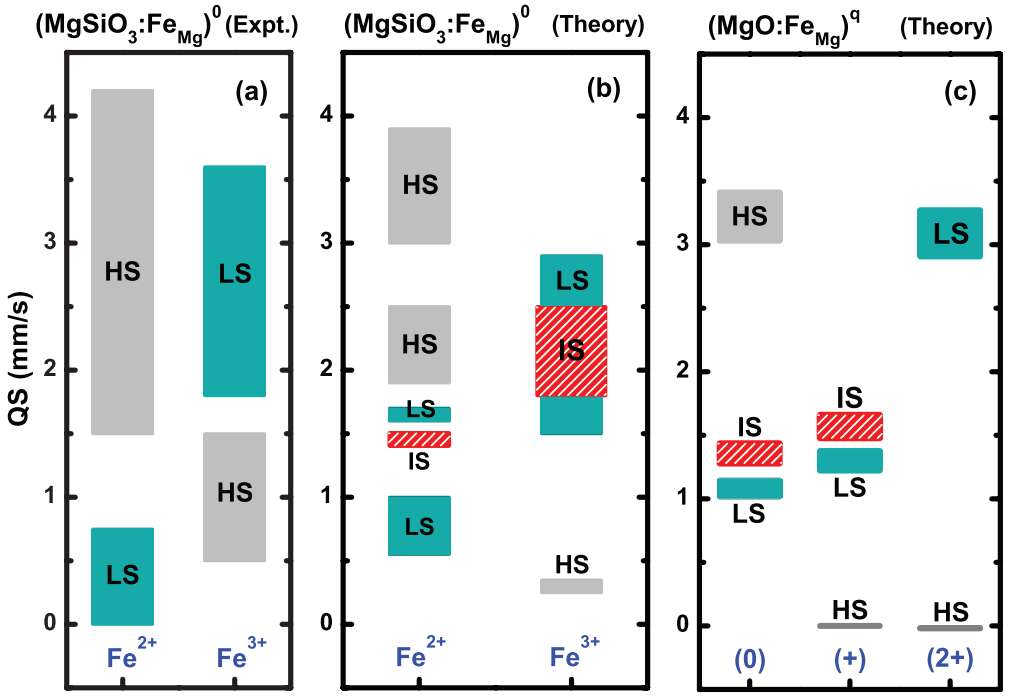

FIG. 8. (Color online) Our theoretical results (c) for the QS in $(MgO : Fe_{Mg})^q$ ($q = 0$, +, or 2+) for zero pressure, compared to experimental[43] (a) and theoretical[42] (b) QS values at the Fe atom in ferrosilicate perovskite, $(MgSiO_3 : Fe_{Mg})^0$. In ferrosilicate perovskite, Fe can have 2+ or 3+ oxidation charge states.

suggesting that same oxidation charge state for iron in MgO. Finally, the $(MgO : Fe_{Mg})^{2+}$ center has QS values for spin states that resemble the ones of the $(MgO : Fe_{Mg})^{+}$ center. This suggests that iron in the $(MgO : Fe_{Mg})^{2+}$ center has a 3+ oxidation charge state, and not a 4+, as it could be expected by a simple inspection. All those results indicate similarities in the properties of iron atoms in MgO or ferropericlase with those in ferrosilicate perovskite. Such similarities of iron in those two materials are not fortuitous, they indicate that the d-related (iron) orbital occupancy plays a major role on the properties of those centers, even more important than the center symmetry or the number of neighboring oxygen atoms.

IV. SUMMARY

In summary, we performed a first-principles investigation on the properties of substitutional iron impurities in magnesium oxide. We found that those centers can stay stable in three charge states: neutral, positive and doubly positive ones. The center in neutral charge state controls the top part of the band gap in HS and LS states. For the lower mantle properties, in which iron is incorporated in ferropericlase alloys, this property should be discussed, since the Fermi level, which depends on the amount of available carriers in the system, is determined by the concentrations of other intrinsic and extrinsic defects, such as vacancies, interstitials, dislocations, and impurities.

We also found that the controlling mechanism of spin transition is associated to the energy barrier between the different spin states. Additionally, we found that there are three possible spin states for the iron in neutral charge state, consistent with results for the iron spin states in ferrosilicate perovskite. The intermediate spin state, with $S = 1$, is a metastable configuration that could be observed in MgO in minor concentrations by EPR or Mösbauer spectroscopy. Additionally, our calculations on the quadrupole splitting indicated similarities of iron atoms in ferropericlase and ferrosilicate perovskite. All those aspects should be discussed in the context of the studies on the charge and radiative conductivity of the lower mantle, with important geophysical implications for the temperature profile of the inner layers of the Earth.

ACKNOWLEDGMENTS

The authors acknowledge partial support from Brazilian agencies FAPESP and CNPq. The authors thank W. V. M. Machado for fruitful discussions.

[1] J. Badro, G. Fiquet, F. Guyot, J. P. Rueff, V. V. Struzhkin, G. Vankó, and G. Monaco, Science **300**, 789 (2003).
[2] J. Badro, J. P. Rueff, G. Vankó, G. Monaco, G. Fiquet, and F. Guyot, Science **305**, 383 (2004).
[3] J. F. Lin, V. V. Struzhkin, S. D. Jacobsen, M. Y. Hu, P. Chow, J. Kung, H. Z. Liu, H. K. Mao, and R. J. Hemley, Nature (London) **436**, 377 (2005).
[4] S. Speziale, A. Milner, V. E. Lee, S. M. Clark, M. P. Pasternak, and R. Jeanloz, Proc. Natl. Acad. Sci. USA **102**, 17918 (2005).
[5] A. F. Goncharov, V. V. Struzhkin, and S. D. Jacobsen, Science **312**, 1205 (2006).
[6] T. Tsuchiya, R. M. Wentzcovitch, C. R. S. da Silva, and S. de Gironcoli, Phys. Rev. Lett. **96**, 198501 (2006).
[7] J. F. Lin, G. Vankó, S. D. Jacobsen, V. Iota, V. V. Struzhkin, V. B. Prakapenka, A. Kuznetsov, and C. S. Yoo, Science **317**, 1740 (2007).
[8] C. McCammon, I. Kantor, O. Narygina, J. Rouquette, U. Ponkratz, I. Sergueev, M. Mezouar, V. Prakapenka, and L. Dubrovinsky, Nat. Geosci. **1**, 684 (2008).
[9] R. M. Wentzcovitch, J. F. Justo, Z. Wu, C. R. S. da Silva, D. A. Yuen, and D. Kohlstedt, Proc. Natl. Acad. Sci. USA **106**, 8447 (2009).
[10] Z. Wu, J. F. Justo, C. R. S. da Silva, S. de Gironcoli, and R. M. Wentzcovitch, Phys. Rev. B **80**, 014409 (2009).
[11] P. J. Tackley, Earth Sci. Rev. **110**, 1 (2012).
[12] J. C. Crowhurst, J. M. Brown, A. F. Goncharov, and S. D. Jacobsen, Science **319**, 451 (2008).
[13] H. Marquardt, S. Speziale, H. J. Reichmann, D. J. Frost, F. R. Schilling, and E. J. Garnero, Science **324**, 224 (2009).
[14] H. Marquardt, S. Speziale, H. J. Reichmann, D. J. Frost, and F. R. Schilling, Earth Planet. Sci. Lett. **287**, 345 (2009).
[15] D. Antonangeli, J. Siebert, C. M. Aracne, D. L. Farber, A. Bosak, M. Hoesch, M. Krisch, F. J. Ryerson, G. Fiquet, and J. Badro, Science **331**, 64 (2011).
[16] H. Keppler, I. Kantor, and L. S. Dubrovinsky, Am. Mineral. **92**, 433 (2007).
[17] J. F. Lin, Z. Mao, I. Jarrige, Y. M. Xiao, P. Chow, T. Okuchi, N. Hiraoka, and S. D. Jacobsen, Am. Mineral. **95**, 1125 (2010).
[18] T. Komabayashi, K. Hirose, Y. Nagaya, E. Sugimura, and Y. Ohishi, Earth Planet. Sci. Lett. **297**, 691 (2010).
[19] P. Blaha, K. Schwarz, G. Madsen, D. Kvaniscka, and J. Luitz, in WIEN2K, *An Augmented Plane Wave Plus Local Orbitals Program for Calculating Crystal Properties*, edited by K. Schwarz (Technical Universitt Wien, Vienna, Austria, 2001).
[20] J. P. Perdew, K. Burke, and M. Ernzerhof, Phys. Rev. Lett. **77**, 3865 (1996).
[21] V. I. Anisimov, J. Zaanen, and O. K. Andersen, Phys. Rev. B **44**, 943 (1991).
[22] G. K. H. Madsen and P. Novák, Europhys. Lett. **69**, 777 (2005).
[23] L. V. C. Assali, W. V. M. Machado, and J. F. Justo, Phys. Rev. B **69**, 155212 (2004).
[24] L. V. C. Assali, W. V. M. Machado, and J. F. Justo, Appl. Phys. Lett. **89**, 072102 (2006).
[25] T. Mattila and A. Zunger, Phys. Rev. B **58**, 1367 (1998).
[26] F. Ayres, L. V. C. Assali, W. V. M. Machado, and J. F. Justo, Appl. Phys. Lett. **88**, 11918 (2006).
[27] R. Larico, J. F. Justo, W. V. M. Machado, and L. V. C. Assali, Phys. Rev. B **79**, 115202 (2009).
[28] L. V. C. Assali, W. V. M. Machado, and J. F. Justo, Phys. Rev. B **84**, 155205 (2011).
[29] K. Persson, A. Bergtson, G. Ceder, and D. Morgan, Geophys. Res. Lett. **33**, L16306 (2006).
[30] M. Cococcioni and S. de Gironcoli, Phys. Rev. B **71**, 035105 (2005).
[31] M. Blanchard, M. Lazzeri, F. Mauri, and E. Balan, Am. Miner. **93**, 1019 (2008).
[32] H. S. Nabi, R. J. Harrison, and R. Pentcheva, Phys. Rev. B **81**, 214432 (2010).

[33]F. Ibrahim and M. Alouani, Phys. Rev. B **85**, 174411 (2012).
[34]*Semiconductors, Physics of Group IV Elements and III-V Compounds*, edited by O. Madelung, M. Shulz, and H. Weiss, Landolt-Börnstein, New series, Group III, Vol. 17 (Springer, New York, 1982).
[35]B. B. Karki, L. Stixrude, S. J. Clark, M. C. Warren, G. J. Ackland, and J. Crain, Am. Miner. **82**, 51 (1997).
[36]I. Kantor, L. Dubrovinsky, C. McCammon, G. Steinle-Neumann, A. Kantor, N. Skorodumova, S. Pascarelli, and G. Aquilanti, Phys. Rev. B **80**, 014204 (2009).
[37]A. Jain, G. Hautier, S. P. Ong, C. J. Moore, C. C. Fischer, K. A. Persson, and G. Ceder, Phys. Rev. B **84**, 045115 (2011).
[38]Y. W. Fei, L. Zhang, A. Corgne, H. Watson, A. Ricolleau, Y. Meng, and V. Prakapenka, Geophys. Res. Lett. **34**, L17307 (2007).
[39]T. Yoshino, E. Ito, T. Katsura, D. Yamazaki, S. M. Shan, X. Z. Guo, M. Nishi, Y. Higo, and K. Funakoshi, J. Geophys. Res. **116**, B04202 (2011).
[40]S. A. Centoni, B. Sadigh, G. H. Gilmer, T. J. Lenosky, T. D. de la Rubia, and C. B. Musgrave, Phys. Rev. B **72**, 195206 (2005).
[41]H. M. Petrilli, P. E. Blöchl, P. Blaha, and K. Schwarz, Phys. Rev. B **57**, 14690 (1998).
[42]H. Hsu, P. Blaha, M. Cococcioni, and R. M. Wentzcovitch, Phys. Rev. Lett. **106**, 118501 (2011).
[43]J. F. Lin, E. E. Alp, Z. Mao, T. Inoue, C. McCammon, Y. M. Xia, P. Chow, and J. Y. Zhao, Am. Miner. **97**, 592 (2012).